JMEPEG (2012) 21:463–470
DOI: 10.1007/s11665-011-9974-4

1059-9495/$19.00

Design of Nano-Micro-Composite Ceramic Tool and Die Material with Back Propagation Neural Network and Genetic Algorithm

Jingjie Zhang, Chonghai Xu, Mingdong Yi, and Bin Fang

(Submitted July 25, 2010; in revised form April 27, 2011)

An algorithm combined with back propagation neural network (BPNN) and genetic algorithm (GA) was used in the optimum design of the compositions of an advanced $ZrO_2/TiB_2/Al_2O_3$ nano-micro-composite ceramic tool and die materials. GA was used to fully optimize the network topology, thresholds, and initial connection weights of BPNN. The input parameters are the contents of each compositions of ceramic tool and die materials and the output parameters are mechanical properties including hardness, flexural strength, and fracture toughness. The compositions with optimum mechanical properties can be chosen for materials preparation with less error and the result can be used to guide the experimental process. As a result, the nano-micro-composite ceramic tool and die material with good mechanical properties was then fabricated. It indicated that the algorithm can offer a robust and efficient way for the compositional design of ceramic tool and die materials.

Keywords material selection, modeling processes, structural ceramics

1. Introduction

In recent years, ceramic tool and die materials such as Al_2O_3, Si_3N_4, Sialon, etc. have got more and more applications in the field of both metal cutting and plastic forming because of their premium properties such as high hardness, wear resistance, and heat resistance. However, the brittleness has limited their further application. ZrO_2 ceramics, with good physical and chemical properties and excellent mechanical properties especially the fracture toughness, have become one of the research hotspots in the field of ceramic materials. Especially in recent years, researchers had fabricated the ZrO_2/WC nanocomposite ceramic material by hot pressing (HP) technique. The highest flexural strength is 1551 MPa when the volume fraction of WC is 20% (Ref 1, 2). While for the ZrO_2/TiB_2 composite ceramic material with the content of 30% TiB_2, the corresponding hardness, flexural strength, and fracture toughness is 13-14 GPa, 1000 MPa, and 8 MPa·$m^{1/2}$, respectively (Ref 3). Some researchers studied the mechanical properties of Al_2O_3-15 wt.% ZrO_2 ceramic composites. The fracture toughness and flexural strength reached 932 MPa and 8.5 MPa·$m^{1/2}$, respectively (Ref 4).

Jingjie Zhang, Chonghai Xu, and **Bin Fang**, School of Mechanical Engineering, Shandong Polytechnic University, Jinan 250353, People's Republic of China; and **Chonghai Xu** and **Mingdong Yi**, School of Mechanical Engineering, Shandong University, Jinan 250061, People's Republic of China. Contact e-mails: xch@spu.edu.cn.

At present, the main research method for ceramic materials is still the traditional "trial-error" method which needs a large number of experiments to determine the optimum material compositions. This traditional method requires researchers to repeat experiments and to face to the complex preparation processes as well as the high cost of the experiment, and so on. Therefore, the utilization of advanced and even intelligent design technologies for ceramic material design is extremely necessary.

The computational intelligence (CI) technique, as an offshoot of artificial intelligence (AI), has provided an effective way to solve some kinds of problems. It is a kind of heuristic algorithm including three categories: neural network, fuzzy system, and evolutionary computation. Genetic algorithm (GA) and artificial neural network (ANN) are the two important CI techniques.

In recent, the two kinds of techniques especially ANN have got successful application in material design of ceramics, etc. For instance, some researchers used ANN to predict the functional properties of ceramic materials from compositions (Ref 5), the bending strength and hardness of particulate-reinforced Al-Si-Mg aluminum matrix composites (Ref 6), the mechanical properties of ceramic tool (Ref 7) or the percentage of alumina in Al_2O_3/SiC ceramic cakes and the pore volume fraction (Ref 8), etc. ANN is a kind of self-learning technology and back propagation neural network (BPNN) is one of the simply and commonly used network architectures. BPNN is based on the gradient descent method where connection weights and thresholds are modified in a direction corresponding to the negative gradient of a backward-propagated error (Ref 9).

Although BPNN has an advantage of high accuracy, it is often plagued by the local minimum point, low convergence or oscillation effects. Therefore, two problems still exist in the application of BPNN. One is the determination of the network topology, especially the neuron number in the hidden layer without the guidance of theoretical formula. The other is the problem of convergence accuracy, i.e., how to determine a

reasonable number of hidden layer and hidden layer neurons to achieve both the required accuracy and short-training time.

In order to overcome the disadvantage of BPNN, GA is usually used for the optimization of BPNN. GA has a strong searching capability and high probability in finding the global optimum solution which is suitable for the early stage of data searching. Although these two techniques seem quite different in the number of involved individuals and the process scheme, they can do a synergistic combination to provide more power of problem solving than either alone (Ref 10-12). Therefore, many researchers have attempted to combine the two algorithms together in order to achieve the complementary advantages (Ref 13, 14).

In this article, a combinational algorithm of BPNN and GA is used for the compositional design of an advanced $ZrO_2/TiB_2/Al_2O_3$ nano-micro-composite ceramic tool and die material.

2. Combinational Algorithm of GA and BPNN

The commonly used combination of GA and BPNN mainly has three methods. One is using GA to optimize the network topology of BPNN which is marked as GA-BP I here; the second is using GA to identify the initial connection weight and threshold which is marked as GA-BP II; while the third is using GA not only to identify the initial connection weight and threshold, but also to optimize the network topology of BPNN which is marked as GA-BP III. Since the algorithm of GA-BP I is the simplest algorithm with lower accuracy of prediction, the latter two kinds of algorithms are further discussed in the present study. Some successful examples of the combination of GA and BPNN (GA-BP II and GA-BP III) have been reported to optimize successfully the flow stress of 304 stainless steel under cold and warm compression (Ref 15), the surface roughness in end milling Inconel 718 (Ref 16) or the plasma processes (Ref 17), etc. In addition, some researchers successfully used the BPNN and combinational algorithms to forward and reverse mappings in green sand mold system (Ref 18) or modeling of TIG welding process (Ref 19), the results both show that combinational algorithm outperforms the BPNN.

2.1 The Algorithm of GA-BP II

BPNN is very sensitive to the initial vectors and different initial values may lead to completely different results. Especially in the specific calculation process, the related initial values are usually determined randomly or by experience. Once the initial value is not properly determined, it will lead to the effect of oscillation or seldom convergence. Even if it is convergent, the process will be quite slow because of the too long time of training or falling into local minimum. And the best connection weight distribution cannot be achieved. Using GA to optimize the connection weights and thresholds of BPNN (GA-BP II) can solve the kind of problem.

The principle of the GA-BP II algorithm is as follows: using GA to optimize the connection weights and thresholds of BPNN from its searching space which contains all the available individuals. Then, the BPNN is trained with these connection weights and thresholds so that the difference between BPNN actual output and target output can be reduced.

Most of the research literatures focus on the utilization of various improved GA to train the connection weights and thresholds of BPNN ignoring the importance of the network topology and its close relationship with the network topology and connection weights. In the present study, a combinational algorithm of BPNN and GA (GA-BP III) is used for the compositional optimum design of nano-micro-composite ceramic tool and die materials. In this algorithm, GA is used to fully optimize BPNN including the comprehensive optimization of the network topology, the initial connection weights, and thresholds.

2.2 The Algorithm of GA-BP III

It is reported that the BPNN network topology can greatly affect the network processing capabilities. Redundant nodes and connections are not allowed existing in a good network topology. However, the design of the network topology has not rigorous and systematic theoretical guidance and remains largely dependent on a person's experience. Using GA to solve the optimization problem of the network topology can be transformed into the process of biological evolution that can be obtained through the selection, crossover and mutation, etc.

According to the Kolmogorov theorem (Ref 20, 21), for three-layer BPNN, it can achieve any given mapping. When the number of the hidden layer neurons is enough, it can use any degree of accuracy to approximate any nonlinear mapping. The neurons in the input layer and output layer are determined on the specific problem; only the number of neurons in the hidden layer is variable. Thus, how to determine the number of the hidden layer neurons has become a very important issue which is the optimum object of the neural network topology. If the number of the neurons in the hidden layer is too little, the network may not be trained satisfyingly with the results, or the network is not robust enough with the poor fault-tolerance. Otherwise, they will make learning time too long and the error is not necessarily the smallest. Hence, there exist an optimal number of the hidden layer neurons.

It is assumed that the neural network is hierarchically fully connected and only the neurons of two adjacent layers are possible to be connected and must be connected. If the input and output vector values are in the real number space and there are no effects between the two connected neurons, the weight of the two connected neurons will be zero. Under the known condition of the input and output neurons, the number of the neurons in the hidden layer can only correspond to the number of the connection weight.

Thus, the principle of the GA-BP III algorithm is as following: before the optimization, GA is used to optimize the number of connection weights, the best connection weight and threshold for BPNN from its searching space which contains all the available individuals. After that, a global optimum solution can be achieved. Then, the last generation of individuals is decoded and the corresponding BPNN network topology, initial connection weights, and thresholds can be achieved. With these values worked as the BPNN network topology and the initial value, samples can then be trained to obtain the final optimal results. A flow chart of GA-BP III algorithm is shown in Fig. 1.

2.3 Process of GA-BP III Algorithm

2.3.1 Encoding. For the BPNN with *n-d-m* three layer, where *n* is the number of neurons of the input layer, *d* is the number of neurons of the hidden layer, and *m* is the number of neurons of the output layer, the floating-point type numbers are used for the connection weights and thresholds to be encoded.

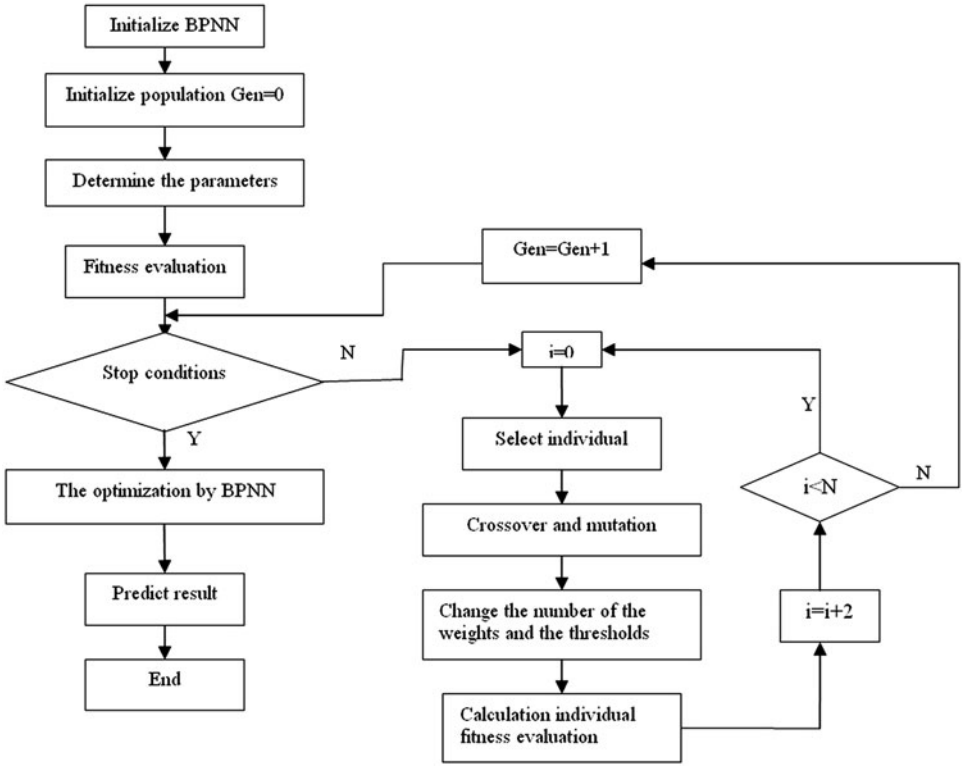

Fig. 1 The flow chart of GA-BP III algorithm

The encoding is linked together to be a long string by the sequence of connection weights and thresholds. Then, the length of the string is:

$$L = n \times d + d + d \times m + m \quad \text{(Eq 1)}$$

The scope of d can be ascertained by the empirical formula of the hidden layer neurons (Ref 22) given below:

$$d = \sqrt{n+m} + \alpha, \quad \text{(Eq 2)}$$

where n and m can be determined based on the actual problem, α is a constant in the range of 1-10. Thus, once the length of the string L is determined, the number of hidden layer neurons and then the network topology of BPNN can be determined. The individual values after decoding are the corresponding connection weights and thresholds.

2.3.2 Determination of the Fitness Function. The relationship between the input and output of the network is available as following (Ref 23):

$$Y_k = \sum_{j=1}^{d} V_{jk} \cdot f\left[\sum_{i=1}^{n} W_{ij} \cdot X_i + \theta_j\right] + r_k \quad \text{(Eq 3)}$$

where f is the transfer function between layers, X_i is the actual input of the neuron i of the input layer, W_{ij} is the connection weight from the neuron i of the input layer to the neuron j of the hidden layer, θ_j is the threshold of the neuron j of the hidden layer, V_{jk} is the connection weight from the neuron j of the hidden layer to the neuron k of the output layer, r_k is the threshold of the neuron k of the output layer, and Y_k is the actual output of the neuron k of the output layer. According to the error between the actual output and the target output, the least-squares error function E can be defined as (Ref 23):

$$E(W, V, \theta, r) = \frac{1}{2p}\sum_{q=1}^{p}\sum_{i=1}^{m}\left(T_i^q - Y_i^q\right)^2, \quad \text{(Eq 4)}$$

where p is the total number of training samples, T_i^q and Y_i^q is the target output and the actual output of the neuron i of the input layer, respectively, when the qth training sample trains.

In order to integrate GA and BPNN, the fitness function of GA is selected as following (Ref 23):

$$f(W, V, \theta, r) = \frac{1}{E(W, V, \theta, r) + 1} \quad \text{(Eq 5)}$$

In this way, once the outputs are available through the BPNN computation, the related outputs are transferred to the fitness function for the comparison and determination of the final value. While the fitness are being updated from generation to generation, a new generation of the population will be produced and do the same evaluation. When the fitness of the population reaches the maximum, the output error of the network becomes the minimum. This process will continue until the end of predetermined generations.

2.3.3 BPNN Modeling. The hardness, flexural strength, and fracture toughness are the main mechanical properties of ceramic tool and die materials. When the processing techniques are determined, the mechanical properties of ceramic tool and die material are mainly decided by the compositions. Therefore, the inputs of the neural network model are the contents of each composition and the outputs are the three mechanical properties of the given materials. Hence, the model has three output neurons.

For the selected $ZrO_2/TiB_2/Al_2O_3$ nano-micro-composite ceramic tool and die material, the BPNN model is then established which has three input neurons (volume fractions of

ZrO_2, TiB_2, and Al_2O_3, respectively) and three output neurons. With the substitution of the number of neurons of the input layer and the number of neurons of the output layer into Eq 1, the string length is $L = 3+7d$. The scope of the number of neurons of the hidden layer is then determined as 4-13 according to Eq 2. The sigmoid-type transfer function is adopted for the input layer to the hidden layer and the linear-type transfer function is adopted for the hidden layer to the output layer.

3. Experimental

The nano-micro-composite ceramic tool and die material $ZrO_2/TiB_2/Al_2O_3$ was fabricated with the vacuum HP technique. High purity nanometer-sized ZrO_2 and micrometer-sized TiB_2 and Al_2O_3 powders were used as the starting materials with average sizes of 39 nm, 1.5 and 1.0 μm, respectively. According to the required volume fraction, the raw material powders were blended. The mixtures were subsequently homogenized with absolute alcohol media and polyethylene glycol (PEG) in a ball mill for 48 h. After milling the slurry was dried in vacuum and screened.

Samples were then formed by vacuum HP technique under the HP temperature of 1445 °C, pressure of 30 MPa, and time duration of 60 min. Sintered bodies were cut with a diamond wheel into samples of $3 \times 4 \times 30$ mm. The flexural strength was measured in an electronic universal testing machine (model INSTRON-5569) by means of the three-point bending method with a span of 20 mm and loading rate of 0.5 mm/min. The Vickers hardness was tested by the testing machine (model Hv-120) with a load of 196 N and a holding time of 15 s. The fracture toughness was determined by the indentation method. The experimental data are listed in Table 1, where H_E, σ_E, and K_{ICE} is the experimental value of hardness, flexural strength, and fracture toughness, respectively. The microstructure was observed with environmental scanning electron microscope (ESEM, model FEI-quanta 200).

4. Results and Discussion

4.1 Simulation Results of GA-BP III Algorithm

According to the principle of GA-BP III algorithm, the corresponding computing process is programmed and run with MATLAB 7.0 software. The corresponding parameters are set as following: the initial population number $N = 30$, the cross probability $P_c = 0.8$, the mutation probability $P_m = 0.1$, and the error $e = 0.001$. When the error reaches the intended target, the training process of BPNN will stop.

In the process of GA optimization, with the increase of the evolution of generation, the fitness and sum-square error is becoming convergent and finally achieves the best value, respectively. At this stage, the corresponding connection weights and thresholds of the neural network become the optimum. Their individuals are decoded as follows: −0.33, 1.00, 0.00, −0.64, −0.09, 0.18, −0.61, −0.38, 0.13, −0.27, −0.27, 0.91, −0.55, 0.72, 0.57, 0.33, −0.48, 0.36, −0.51, −0.19, −0.19, −0.05, 0.13, −0.32, −0.52, 0.24, −0.78, 0.29, 0.39, 0.13, −0.46, 0.00, 0.00, 0.47, 1.00, −0.32, −0.59, 0.36, −0.07, −0.40, −0.34, −0.28, −0.22, −1.00, −0.28, −0.61, 0.19, 0.49, −0.82, 0.00, 0.10, 0.52, 0.63, −0.48, 0.96, −0.89, 0.23, 0.11, −0.59. According to the string length $L = 3+7d$ and with the number of the above parameters as the string length which is 59, the number of hidden layer neurons is ascertained as 8. Therefore, the BPNN network topology is 3-8-3 and the thresholds are the last 11 parameters in the decoded individuals listed above. Some connection weights in the list above are found to be 0.00 which indicates that the connection between the two neighboring neurons is invalid.

The concrete network topology of GA-BP III algorithm is shown in Fig. 2. It can be seen that the first neuron of input

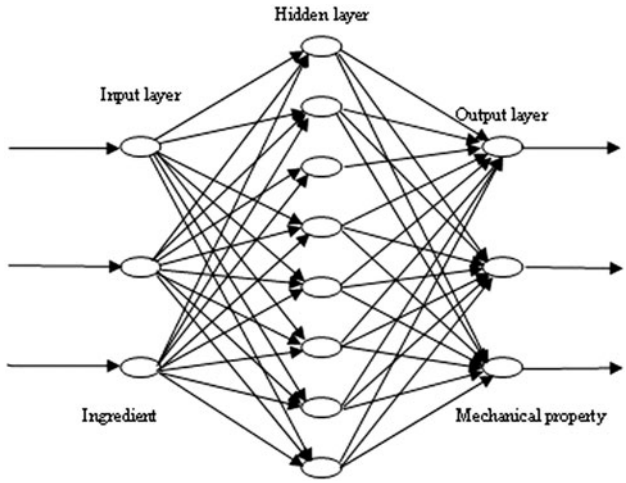

Fig. 2 The BPNN network topology for GA-BP III algorithm

Table 1 The training samples for GA-BP III simulation

Sample number	Volume fraction of ZrO_2 V_{ZrO_2}, vol.%	Volume fraction of TiB_2 V_{TiB_2}, vol.%	Volume fraction of Al_2O_3 $V_{Al_2O_3}$, vol.%	Hardness H_E, GPa	Flexural strength σ_E, MPa	Fracture toughness K_{ICE}, MPa·m$^{1/2}$
1	90	5	5	10.03	618.91	9.76
2	85	5	10	10.20	501.29	10.59
3	80	5	15	10.36	508.86	9.95
4	85	10	5	10.37	616.81	10.51
5	80	10	10	10.71	612.05	11.37
6	75	10	15	10.19	564.78	12.20
7	80	15	5	9.82	512.95	7.86
8	75	15	10	10.22	523.92	7.91
9	70	15	15	10.14	520.36	8.11

Table 2 The predicted results of GA-BP III algorithm

Predicted number	Volume fraction of ZrO_2 V_{ZrO_2}, vol.%	Volume fraction of TiB_2 V_{TiB_2}, vol.%	Volume fraction of Al_2O_3 $V_{Al_2O_3}$, vol.%	Hardness H_p, GPa	Flexural strength σ_p, MPa	Fracture toughness K_{ICP}, MPa·m$^{1/2}$
1	85	6	9	10.4052	581.2162	10.3338
2	85	7	8	10.6214	652.4133	10.2449
3	85	8	7	10.7445	684.5087	10.3756
4	85	9	6	10.6831	674.3180	10.4994
5	80	6	14	10.5760	525.4235	10.7261
6	80	7	13	10.6851	536.8278	11.2773
7	80	8	12	10.7196	547.2214	11.6317
8	80	9	11	10.7194	567.6776	11.7215
9	80	11	9	10.6646	661.8577	10.6589
10	80	12	8	10.4706	656.7249	9.9358
11	80	13	7	10.1025	590.1572	9.1546
12	80	14	6	9.8855	537.7169	8.3906
13	75	11	14	10.3267	539.3551	11.4096
14	75	12	13	10.4194	518.8999	10.5038
15	75	13	12	10.4649	509.9802	9.6927
16	75	14	11	10.4339	517.1729	8.9028
17	60	10	30	9.73674	566.5057	7.3339
18	60	15	25	9.74865	566.6555	7.2675
19	60	20	20	9.76026	566.9639	7.2397
20	60	25	15	9.05516	406.9483	7.0475
21	60	30	10	9.76318	506.0931	5.7454

layer and the third neuron of hidden layer is no connection. The third neuron of hidden layer and the second and the third neurons of output layer are also connectionless. The data within the range of the experimental results are selected as the data for prediction in order to get the optimum compositions corresponding to the best mechanical properties. The predicted results of GA-BP III algorithm are shown in Table 2, where H_P, σ_P, and K_{ICP} are the predicted hardness, flexural strength, and fracture toughness, respectively. It indicates that the highest flexural strength is 684.5087 MPa and the highest hardness is 10.7445 GPa with the corresponding volume fractions of 8 vol.% TiB_2 and 7 vol.% Al_2O_3. The fracture toughness with the same compositions is 10.3756 MPa·m$^{1/2}$ which is slightly less than the best value 11.7215 MPa·m$^{1/2}$ when the volume fraction of TiB_2 and Al_2O_3 is 9 and 11%, respectively. While the flexural strength and hardness with the latter compositions is 567.6776 MPa and 10.7194 GPa, respectively. It suggests that comprehensive good mechanical properties of the nano-micro-composite ceramic tool and die material $ZrO_2/TiB_2/Al_2O_3$ can be achieved when the volume fraction of TiB_2 and Al_2O_3 is 8 and 7%, respectively.

After about 100 generations of searching, the fitness and the sum-square error has been stabilized, respectively, as shown in Fig. 3. The curve of BPNN training target is shown in Fig. 4. It indicates that the error can reach the predetermined goal only after eight steps of iteration. The elapsed time is 129.939 s and the mean square error (MSE) is 0.1491.

4.2 Experimental Verification and Discussion

According to the above simulation results of GA-BP III algorithm, 8 vol.% TiB_2 and 7 vol.% Al_2O_3 are chosen as the optimum compositions since material with the ingredients will have the best flexural strength, the best hardness, and better fracture toughness. Then, $ZrO_2/TiB_2/Al_2O_3$ nano-micro-composite ceramic tool and die material with the above

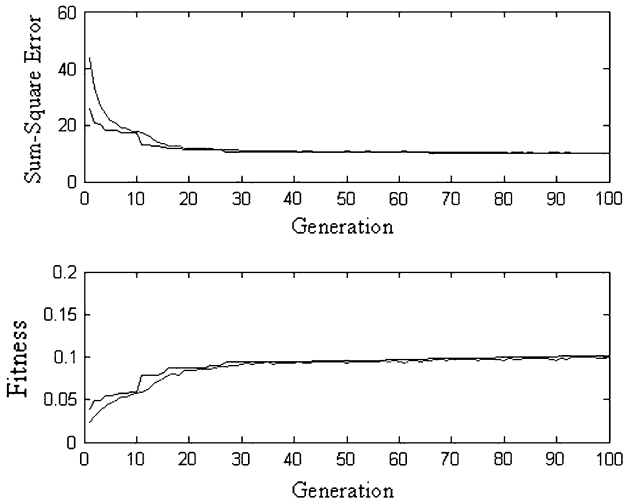

Fig. 3 The curve of sum-square error and fitness of GA-BP III algorithm

optimum compositions was prepared with the vacuum HP technique described in Section 3. Mechanical properties including flexural strength, hardness and fracture toughness were also measured. The simulation results of standard BPNN algorithm and GA-BP II algorithm are also achieved in order for the comparison which is shown in Fig. 5. It indicates that the error can reach the predetermined goal after 61 steps of iteration. The corresponding MSE is 1.2390. For the GA-BP II algorithm, after about 100 generations of searching, the fitness and the sum-square error has been stabilized as shown in Fig. 6. The curve of BPNN training target of GA-BP II algorithm is shown in Fig. 7. It can be seen that the error can reach the predetermined goal after 12 steps of iteration. The elapsed time is 144.199 s and the MSE is 1.0483. Compared

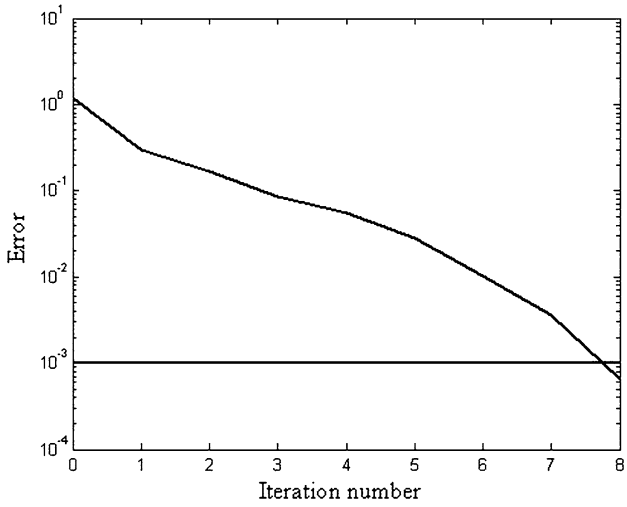

Fig. 4 The curve of BPNN training target of GA-BP III algorithm

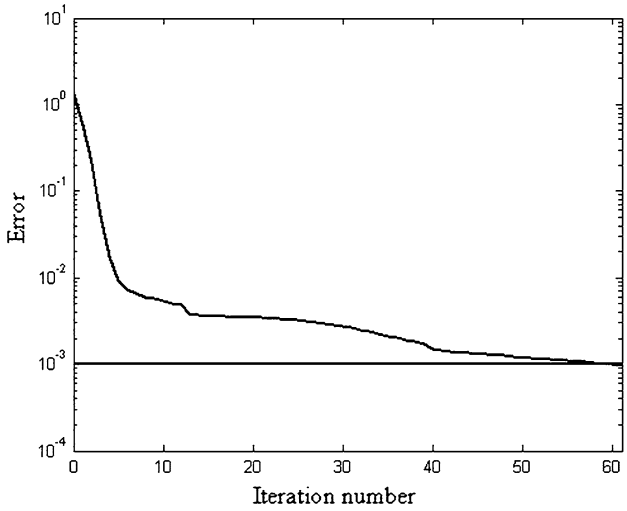

Fig. 5 The curve of BPNN training target of standard BPNN

with the above two algorithms, the GA-BP III algorithm has the least number of iteration steps, shorter elapsed time and smallest MSE.

Both the experimental data and the predicted data of these three kinds of algorithms mentioned above are all listed in Table 3 as well as the relative errors between the predicted and experimental data. It can be seen that the two kinds of the combinational algorithms of both GA-BP II and GA-BP III all have better prediction accuracy than the standard BPNN. However, the GA-BP III algorithm has the least relative error among the three algorithms. The least relative error of the hardness, flexural strength, and fracture toughness for GA-BP III algorithm is 1.8, 1.4, and 0.7%, respectively, which is approximately 38, 20, and 32% of that of GA-BP II algorithm and 20, 19, and 9% of that of standard BPNN. The predicted data of GA-BP III algorithm better coincide with the experimental data and have high accuracy of prediction. Therefore, it can well be used in the compositional design of ceramic tool and die materials with high accuracy of prediction and reliability.

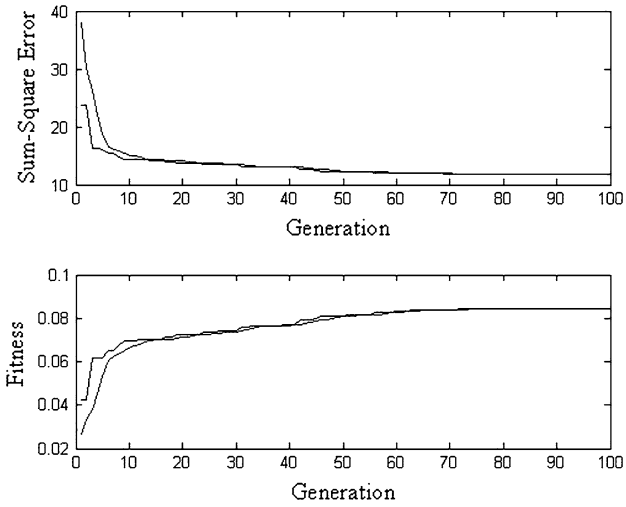

Fig. 6 The curve of sum-square error and fitness of GA-BP II algorithm

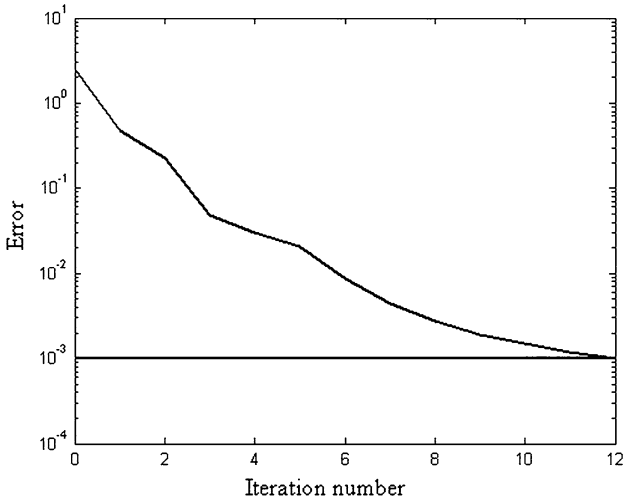

Fig. 7 The curve of BPNN training target of GA-BP II algorithm

After the compositional design and fabrication of ZrO_2/TiB_2/Al_2O_3 nano-micro-composite ceramic tool and die material, the corresponding microstructural morphologies of the material with different compositions were analyzed with scanning electronic microscope (SEM). The typical SEM morphology of ZrO_2/TiB_2/Al_2O_3 nano-micro-composite ceramic tool and die material with the optimum compositions is shown in Fig. 8. It indicated that both TiB_2 and Al_2O_3 grains were distributed uniformly in the ZrO_2 matrix. The fracture mode of the composite material was the mixture of transgranular and intergranular fracture. While for those materials with non-optimum compositions, the phenomena of either low density or abnormally grown grains were usually observed. Besides the main toughening mechanism of phase transformation from ZrO_2, crack deflection, crack bridging, crack branching, etc. contributed simultaneously to the enhancement of the fracture toughness (Ref 24).

The ceramic composites were then used in the friction and wear tests (Ref 24). Lower coefficient of friction and higher wear resistance had been achieved compared with that of pure ZrO_2 ceramic. It suggests that the developed ZrO_2/TiB_2/Al_2O_3

Table 3 Comparison of the predicted and experimental results of the ZrO_2-based ceramic composite with 8 vol.% TiB_2 and 7 vol.% Al_2O_3

	Hardness *H*, GPa	Relative error Δ, %	Flexural strength σ, MPa	Relative error Δ, %	Fracture toughness K_{IC}, MPa·m$^{1/2}$	Relative error Δ, %
Experimental	10.95	···	694.4	···	10.3	···
Standard BPNN	9.9439	9.2	643.1057	7.4	11.1386	8.1
GA-BP II	10.4304	4.7	644.8852	7.1	10.0741	2.2
GA-BP III	10.74452	1.8	684.5087	1.4	10.3756	0.7

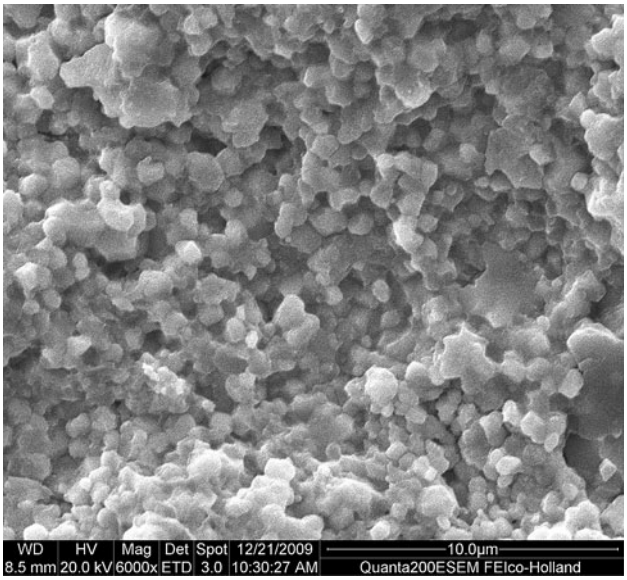

Fig. 8 SEM morphology of $ZrO_2/TiB_2/Al_2O_3$ nano-micro-composite ceramic tool and die material with the optimum compositions

nano-micro-composite ceramic tool and die material will have prospective applications in the fields of drawing and extrusion of non-ferrous metals such as copper and aluminum.

5. Conclusions

With the utilization of GA-BP III algorithm for the compositional design of nano-micro-composite ceramic tool and die material, the number of steps of iteration, the elapsed time, and the MSE can noticeably be reduced. It can avoid the local minimum problem and can present more accurate and reliable results. Preparation experiments of $ZrO_2/TiB_2/Al_2O_3$ nano-micro-composite ceramic tool and die material indicate that the relative error between the experimental and predicted results of the hardness, flexural strength, and fracture toughness is 1.8, 1.4, and 0.7%, respectively, for the GA-BP III algorithm which is the least relative error among the three kinds of algorithms. The predicted data better coincide with the experimental data and have high accuracy of prediction. Therefore, the GA-BP III algorithm is a kind of the fast, effective, and reliable algorithms in the prediction of mechanical properties of nano-micro-composite ceramic tool and die materials. It suggests that it can also be effectively applied in the material design area of other ceramic composites.

Acknowledgments

This work was supported by the National Basic Research Program of China (Grant No. 2009CB724402), Shandong Provincial Natural Science Foundation for Distinguished Young Scholars, China (Grant No. JQ201014), the National Natural Science foundation of China (Grant No. 51075248), Shandong Provincial Natural Science Foundation, China (Grant No. ZR2009FZ005) and the Program for New Century Excellent Talents in University of China (Grant No. NCET-10-0866).

References

1. G. Anné, S. Put, K. Vanmeensel et al., Hard, Tough and Strong ZrO_2-WC Composites From Nanosized Powders, *J. Eur. Ceram. Soc.*, 2005, **25**, p 55–63
2. D. Jiang, O. Van der Biest, and J. Vleugels, ZrO_2-WC Nanocomposites With Superior Properties, *J. Eur. Ceram. Soc*, 2007, **27**, p 1247–1251
3. B. Basu, Microstructure and Mechanical Properties of ZrO_2-TiB_2 Composites, *J. Mater. Sci.*, 2004, **39**, p 6389–6392
4. P.G. Rao, M. Iwasa, T. Tanaka, I. Kondoh, and T. Inoue, Preparation and Mechanical Properties of Al_2O_3-15 wt.% ZrO_2 Composites, *Scr. Mater.*, 2003, **48**, p 437–441
5. D.J. Scott, P.V. Coveney, J.A. Kilner, J.C.H. Rossing, and N.M. Alford, Prediction of the Functional Properties of Ceramic Materials From Composition Using Artificial Neural Networks, *J. Eur. Ceram. Soc.*, 2007, **27**, p 4425–4435
6. N. Altinkok and R.N. Korker, Neural Network Approach to Prediction of Bending Strength and Hardening Behavior of Particulate Reinforced (Al-Si-Mg) Aluminium Matrix Composites, *Mater. Des.*, 2004, **25**, p 595–602
7. C.Z. Huang, L. Zhang, L. He, J. Sun, B. Fang, and B. Zou, A Study on the Prediction of the Mechanical Properties of a Ceramic Tool Based on an Artificial Neural Network, *J. Mater. Process. Technol.*, 2002, **129**, p 399–402
8. N. Altinkok and R.N. Korker, Mixture and Pore Volume Fraction in Al_2O_3/SiC Ceramic Cake Using Artificial Neural Networks, *Mater. Des.*, 2005, **26**, p 305–311
9. X. Jiang and H. Adeli, Clustering-Neural Network Models for Freeway Work Zone Capacity Estimation, *Int. J. Neural Syst.*, 2004, **14**, p 147–163
10. Y. Gary and H.M. Lu, Hierarchical Genetic Algorithm for Near-Optimal Feedforward Neural Network Design, *Int. J. Neural Syst.*, 2002, **12**, p 31–43
11. X. Yao, Evolving Artificial Neural Network, *Proc. IEEE*, 1999, **87**, p 1423–1447
12. M. Gen and R. Cheng, *Genetic Algorithm and Engineering Optimization*, Wiley, New York, 2000
13. R.S. Sexton, R.E. Dorsey, and J.D. Johnson, Toward Global Optimization of Neural Networks: A Comparison of the Genetic Algorithm and Backpropagation, *Decis. Support Syst.*, 1998, **22**, p 171–185
14. J.N.D. Gupta and R.S. Sexton, Comparing Backpropagation with a Genetic Algorithm for Neural Network Training, *Omega*, 1999, **27**, p 679–684
15. S.H.M. Anijdan, H.R. Madaah-Hosseini, and A. Bahrami, Flow Stress Optimization for 304 Stainless Steel Under Cold and Warm Compression by Artificial Neural Network and Genetic Algorithm, *Mater. Des.*, 2007, **28**, p 609–615

16. B. Ozcelik, H. Oktem, and H. Kurtaran, Surface Roughness Inend Milling Inconel 718 by Coupling Neural Network Model and Genetic Algorithm, *Int. J. Adv. Manuf. Technol.*, 2005, **27**, p 234–241
17. B. Kim and J. Bae, Prediction of Plasma Processes Using Neural Network and Genetic Algorithm, *Solid State Electron.*, 2005, **49**, p 1576–1580
18. M. Parappagoudar, D.K. Pratihar, and G.L. Datta, Forward and Reverse Mappings in Green Sand Mould System Using Neural Networks, *Appl. Soft Comput.*, 2008, **8**, p 239–260
19. P. Dutta and D.K. Pratihar, Modeling of TIG Welding Process Using Conventional Regression Analysis and Neural Network-Based Approaches, *J. Mater. Process. Technol.*, 2007, **184**, p 56–68
20. K. Vera, Kolmogorov's Theorem is Relevant, *Neural Comput.*, 1991, **3**, p 617–622
21. Fecit Scitech Research Development Center, *Analysis and Design of Neural Network with MATLAB 6.5*, Electronics Press, Beijing, 2003 (in Chinese)
22. D.Q. Zhu and H. Shi, *The Principle and Application of Artificial Neural Networks*, Science Press, Beijing, 2006 (in Chinese)
23. X.Q. Gu, D.X. Yi, and C.H. Liu, Optimization of Topological Structure and Weight Value of Artificial Neural Network Using Genetic Algorithm, *J. Guangdong Univ. Technol.*, 2006, **23**, p 64–69 (in Chinese)
24. M.D. Yi, "Research and Application of Zirconia Nanocomposite Ceramic Die Material Based on Tribological Design," Master Thesis, Shandong Institute of Light Industry, Jinan, China, 2010 (in Chinese)